Title:
Parametric Analysis for Computational Resource Savings in a New Coating Thickness Model for Robotized Thermal Spraying Processes

Authors:
Chengbiao Wang, 2023125095@chd.edu.cn, Key Laboratory of Road Construction Technology and Equipment of MOE, School of Construction Machinery, Chang'an University
Jiangzhuo Ren, renjz@chd.edu.cn, Key Laboratory of Road Construction Technology and Equipment of MOE, School of Construction Machinery, Chang'an University
Jizhuang Hui, huijz@chd.edu.cn, Key Laboratory of Road Construction Technology and Equipment of MOE, School of Construction Machinery, Chang'an University
Yongsheng Ma, mays@sustech.edu.cn, Department of Mechanical and Energy Engineering, Southern University of Science and Technology

Keywords:
Thermal Spray, Numerical Modeling, Particle ejection probability, Coating thickness modeling, Optimization of computing resources

DOI: 10.14733/cadconfP.2025.229-234

Introduction:

Thermal spraying deposits molten materials onto substrates through high-velocity particle impacts accelerated by pressurized gas, forming dense coatings via rapid deformation and solidification [4]. Coating quality metrics—particularly thickness uniformity—have conventionally required destructive testing and iterative experimental adjustments, incurring prohibitive temporal and material costs [2]. To reduce these costs and accelerate coating development, numerical simulations are used to model the coating formation process, optimizing parameters and enhancing quality. Nonetheless, the process is complex, involving intricate physicochemical changes and a large number of deposited particles [1], which demands significant computational resources, making computational resource optimization a critical challenge in the field.

Over the past two decades, various models, such as the beta, double beta, and Gaussian distribution models [5], have been developed to fit coating growth-rate functions. These models, combined with discretized positional points along the spraying path, are used to simulate coating thickness distribution. However, this approach has limitations, as it does not account for particle deposition, stacking processes, or variations in spray angles and complex substrate geometries, thereby restricting its flexibility.

Therefore, a new coating thickness growth-rate model was developed, incorporating the cross-sectional coating profile to describe the formation process. This model has been comprehensively reviewed in a separate journal article. It begins with particle ejection and approximates particle flight, impact, deformation, and stacking, ultimately constructing a coating thickness growth-rate model. This approach offers greater flexibility and applicability in handling complex workpieces and varying spray angles. However, its computational cost and efficiency require further investigation. Therefore, this study explores key parameters for optimizing computational resource consumption in the coating thickness simulation process.

Main Idea:
It should be emphasized that coating growth is a complex process. In general, the increase in coating thickness results from the formation of molten particles following impact, spattering, deformation, and stacking. Given the complexity of these processes, simulating coating growth requires significant computational power due to the large number of particles involved and the intricate physical and chemical changes during deposition. To address this challenge, the model employs the median particle radius (r) as the equivalent particle dimension, enabling calculation of deposited particle quantities and subsequent evolution simulation. This approach significantly reduces computational load while maintaining physical fidelity through statistical equivalence principles. The complete model construction workflow, including parameter derivation and validation steps, is systematically presented in Fig. 1.

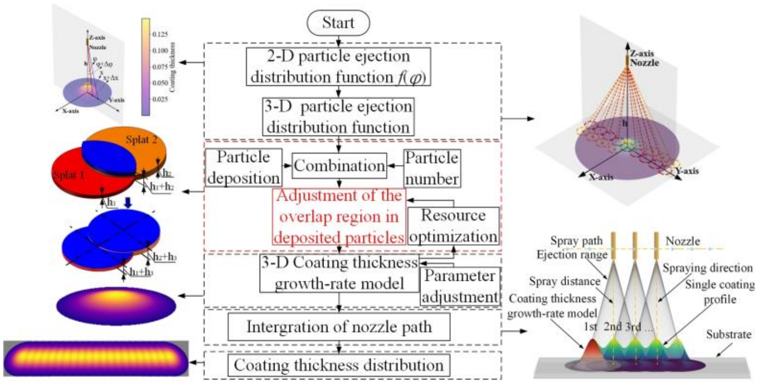

Fig. 1: Over flowchart of the proposed coating thickness distribution modeling.

In the process of constructing the coating thickness distribution model, the experimentally measured coating thickness profile is first fitted to a function $g(x)$, as shown in Eqn. (1). Based on this, the assumed function $f(\varphi)$ at the nozzle exit is derived (Eqn. (2)), from which the 2-D particle ejection distribution function is then calculated.

$$g(x) = a_0 + a_1 x + a_2 x^2 +,...,+ a_n x^n + o(x^n) \tag{1}$$

where, x represents the radial distance from the centerline of the nozzle chamber.

$$f(\varphi) = b_0 + b_1(\varphi - \varphi_0) + b_2(\varphi - \varphi_0)^2 +,...,b_n(\varphi - \varphi_0)^n + R_n((\varphi - \varphi_0)^n) \tag{2}$$

where, φ represents the particle ejection angle relative to the centerline of the nozzle chamber, and $f(\varphi)$ denotes the particle ejection distribution function with respect to the ejection angle φ at the nozzle exit. Since the nozzle chamber is generally rotationally symmetric, φ_0=0 in Eqn. (2), which enables for the determination of the unknown coefficients in Eqn. (2), thereby relating the ejection angle φ to the radial distance, as shown in Eqn. (3).

$$\varphi + \Delta\varphi = \arctan\left(\frac{\Delta x}{h(1+\frac{x}{h}) + (\Delta x + 2h)\frac{x}{h}}\right) + \arctan\frac{x}{h} \tag{3}$$

where, $\Delta\varphi$ represents the change in the ejection angle φ, h denotes the spray distance, and Δx corresponds to the change in radial distance with respect to variations in the ejection angle, as shown in Fig. 1.

Due to the coating profile is continuous and compact, the discretization of the ejection angle depends on the uniform variation of the radial distance, which discretizes the ejection angle φ, as shown in Eqn. (4).

$$\varphi = \arctan\frac{i \times \Delta x}{h}, i \in (-n, n) \tag{4}$$

where, φ_i is the deflection angle value of the i^{th} discretized ejection position, n is a half of the total discretization amount in the ejection range, and the value of n is an integer. Additionally, during the discretization process, Δx is typically set to $2r$.

The 3-D particle ejection distribution is derived by rotating discretized ejection angles about the chamber's axis. To ensure uniform particle deposition on the substrate surface and the continuity of the coating profile, the number of rotation points at different radial distances from the chamber axis is calculated using Eqn. (5)).

$$m_i = \left[\frac{2\pi h \tan\varphi_i}{\Delta l}\right] \tag{5}$$

where, Δl represents the distance between adjacent deposition points, typically set to $2r$, m_i denotes the number of rotation positions at the corresponding ejection angle φ_i, and the positions of each ejection angle in 3-D space are shown in Fig. 1. Next, by normalizing the function values of the ejection angle positions in 3-D space, the probability of particle occurrence at each location can be determined, enabling the investigation of ejection behavior at different ejection angles.

In the subsequent content, the influence of particle deposition and stacking on coating profile growth will be investigated. Given the vast number of particles involved in the coating formation process, simulating multi-particle deposition and deformation requires approximating the impacts and deformations of particles to balance computational resource consumption. Therefore, an equivalent particle deposition model is proposed, as highlighted in the red box in Fig. 1. With the consideration of impact and deformation of adjacent equivalent particles, overlapping area are formed, and the area of these regions can be calculated using Eqn. (6).

$$S_3 = 2(r_{cylinder}^2 \arccos(\frac{d}{2r_{cylinder}}) - \frac{d}{2}\sqrt{4r_{cylinder}^2 - d^2}) \tag{6}$$

where, $r_{cylinder}$ denotes the radius of the equivalent cylinder for the deposited equivalent particles, which is calculated as the product of the equivalent particle's flattening ratio ξ [3] and radius. d represents the distance between the centerlines of adjacent deposition points, while S_3 is the area of the overlapping region between the equivalent cylinders at two adjacent deposition points. The height of the S_3 region is the sum of the cylinder heights of the adjacent particles. Adjacent cylinder overlap approximation (Eqn. (7) and Eqn. (8)) achieves model complexity reduction, coating volume conservation, and computational resource optimization.

$$V_{overlapped} = S_3 \times \min(h_1, h_2) \tag{7}$$

$$h_3 = \frac{V_{overlapped}}{(2\pi r_{cylinder}^2 - S_3)} \tag{8}$$

where h_1 and h_2 represent the heights of the equivalent cylinders between adjacent cylinders, $V_{\text{overlapped}}$ denotes the volume of the overlap between the adjacent equivalent cylinders, and h_3 is the height at which the overlapped volume $V_{\text{overlapped}}$ is distributed between the two adjacent cylinders. The coating thickness growth-rate model is derived by integrating the 3-D particle ejection distribution function, the equivalent particle deposition model, and the number of deposited particles, as shown in Fig. 1.

To obtain the thickness distribution, it is necessary to integrate the spraying path with the coating thickness growth-rate model. As shown in Fig. 1, the spraying path is discretized into a series of points, simulating the nozzle's movement trajectory. For example, by simulating the linear movement of the nozzle, the coating thickness distribution is achieved, as shown at the bottom of Fig. 1.

It is important to emphasize that the coating growth-rate model consists of several modules, including the equivalent particle deposition model and the 3-D particle ejection distribution function. The parameters within these modules are interrelated, and the coating simulation requires a large number of deposited particles, leading to significant resource consumption. Therefore, minimizing and balancing resource usage is a critical challenge addressed in this study. To achieve this, the effects of model setup parameters on the computational resource consumption of the modeling process and model accuracy are analyzed.

During the particle ejection and deposition stacking process, the discrete ejection angle positions φ_i and the number of points n are determined to ensure the continuity of the coating profile. These values can be calculated using Eqn. (4). The positions of the discrete ejection angles further influence the number of deposition points. To achieve a uniform deposition, the number of deposition points m_i at each ejection angle is calculated using Eqn. (5). The discretization of the ejection angle and the number of deposition points are closely linked to the equivalent particle radius. Equivalent particle radius directly relates to the number of deposited particles. In particular, increasing the equivalent particle radius can reduce the effect on the coating profile caused by other parameters, which enhances the continuity of the coating profile to some extent. Additionally, particle's flattening ratio significantly affects the equivalent cylinder radius, which in turn influences the continuity, smoothness, and computational resource consumption of the coating profile. However, to explore the effect of particle radius, a fixed value of the flattening ratio should be set up. In the next section, six coating profiles are simulated with a fixed flattening ratio of 3.6 and varying equivalent particle radius for quantitatively investigating the impact of equivalent particle radius on computational resource consumption and simulation result.

Result and Discussion:

Tab. 1 gives the run times and message usage with different equivalent particle radius. It could also be noted that the values of differential change in the radial distance x (Δx) and arc length between two adjacent deposition point at the same radius (Δl) are associated with the equivalent particle radius.

It is obvious that increasing the equivalent particle radius results in little changes in the cross-sectional coating profile, however, significantly reducing both run time and memory usage. Fig. 2 further shows the plots of the results.

In fact, through the investigations on a number of simulations, the computational resource consumption is strongly determined by the overlapping calculation among adjacent particles. A greater equivalent particle radius means a significant reduce on the overlapping calculation, thus leads to a short rum time and a less message usage.

Coating profile	r(mm)	Δx(mm)	Δl(mm)	ξ	Run time (s)	Message usage (MB)
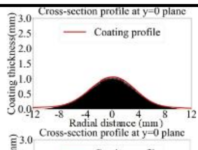	0.006285	0.01257	0.01257	3.6	259.38	6355.57
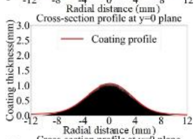	0.0069135	0.013827	0.013827	3.6	184.38	5450.37
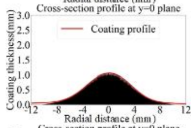	0.007542	0.015084	0.015084	3.6	154.38	4748.14
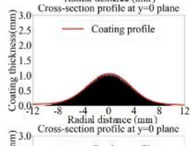	0.0081705	0.016341	0.016341	3.6	132.26	4324.37
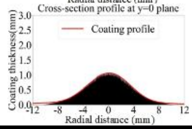	0.008799	0.017598	0.017598	3.6	108.42	3367.08

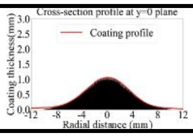	0.0094275	0.018855	0.018855	3.6	85.65	3321.02

Tab. 1: Comparison of resource consumption under different parameters.

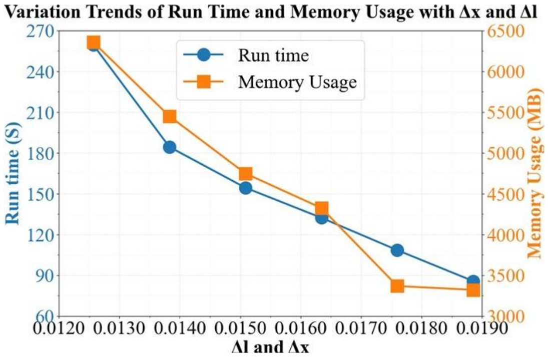

Fig. 2: Computing power resource consumption trend under different parameters.

Conclusions:
This study briefly introduces our new method for modeling coating thickness distribution. By investigating the impact of changes in interrelated parameters (such as particle radius) on run time and memory usage, the result shows that within a specific range of parameter variations, increasing the parameter r can effectively reduce the computational resource consumption with a little effect on the simulated coating profile.

For future work, parameter optimization methods can be employed to generate the most efficient model setup, balancing computational accuracy and time.

Acknowledgments:
This work was supported by the Natural Science Basic Research Program of Shaanxi (#2024JC-YBQN-0438) and Shaanxi Province Qin Chuang yuan Program - Innovative and Entrepreneurial Talents Project (#QCYRCXM-2022-352). The authors would also highlight the support of Shenzhen ESPE-SUSTech Collaboration Project (#K2233Z015 for Y Ma), Guandong provincial support on “Advanced 3D Model Reconstruction and Intelligent Measurement in Manufacturing”, via Fundamental and Applied General Research Regional Fund (Key Project #2023B1515120017 for Y Ma), and the startup funds from SUSTech (#Y01336236 for Y Ma) and Shenzhen city (#Y01336136 for Y Ma).

References:
[1] Li, C.-J.; Yang, G.-J.: Relationships between feedstock structure, particle parameter, coating deposition, microstructure and properties for thermally sprayed conventional and nanostructured WC–Co, International Journal of Refractory Metals and Hard Materials, 39, July 2013, 2-17. https://doi.org/10.1016/j.ijrmhm.2012.03.014.
[2] Ren, J.; Sun, Y.; Hui, J.; Ahmad, R.; Ma, Y.: Coating thickness optimization for a robotized thermal spray system, Robot. Comput.-Integr. Manuf., 83, 2023, 102569. https://linkinghub.elsevier.com/retrieve/pii/S0736584523000455.
[3] Tiamiyu, A.A.; Schuh, C.A.: Particle flattening during cold spray: Mechanistic regimes revealed by single particle impact tests, Surf. Coat. Technol., 403, 2020, 126386. https://doi.org/10.1016/j.surfcoat.2020.126386.
[4] Tejero-Martin, D.; Rezvani Rad, M.; McDonald, A.; Hussain, T.: Beyond traditional coatings: A review on thermal-sprayed functional and smart coatings, Journal of Thermal Spray Technology,

28, 2019, 598-644. https://doi.org/10.1007/s11666-019-00857-1.

[5] Zhong, Y.; Song, L.; Sha, J.; Du, X.; Zhang, G.: Modeling of coating growth rate for digital camouflage robotic spraying based on elliptic double β models, 2024 10th International Conference on Electrical Engineering, Control and Robotics (EECR), Guangzhou, China, IEEE, 2024, 63-68. https://doi.org/10.1109/EECR60807.2024.10607272.